Effect of NaH/MgB_2 ratio on the hydrogen absorption kinetics of the system NaH D MgB_2

Claudio Pistidda [a,*], Daphiny Pottmaier [b], Fahim Karimi [a], Sebastiano Garroni [c], Agnieszka Rzeszutek [a], Martin Tolkiehn [d], Maximilian Fichtner [e], Wiebke Lohstroh [e,f], Marcello Baricco [b], Thomas Klassen [a], Martin Dornheim [a]

[a] Institute of Materials Research, Materials Technology, Helmholtz-Zentrum Geesthacht, Max-Planck-Straße 1, D-21502 Geesthacht, Germany
[b] Department of Chemistry and NIS, University of Turin and INSTM, Via P. Giuria 9, I-10125 Torino, Italy
[c] Dipartimento di Chimica e Farmacia, Universita` di Sassari and INSTM, Via Vienna 2, I-07100 Sassari, Italy
[d] DESY Synchrotron, at the Beam Line D3, Hamburg, Germany
[e] Institute of Nanotechnology, Karlsruhe Institute of Technology, Postfach 3640, 76021 Karlsruhe, Germany
[f] Heinz Maier-Leibnitz Zentrum, Technische Universita¨t Mu¨nchen, Lichtenbergstraße 1, 85747 Garching, Germany

Abstract

In this work the effect of the ratio of starting reactants on the hydrogen absorption reaction of the system xNaH þ MgB_2 is investigated. At a constant hydrogen pressure of 50 bar, depending on the amount of NaH present in the system NaH þ MgB_2, different hydrogen absorption behaviors are observed. For two system compositions: NaH þ MgB_2 and 0.5NaH þ MgB_2, the formation of $NaBH_4$ and MgH_2 as only crystalline hydrogenation products is achieved. The relation between the ratio of the starting reactants and the obtained hydrogenation products is discussed in detail.

Keywords: Hydrogen storage , Boron hydride, Kinetics

1. Introduction

The use of fossil fuels as energy supply is growing increasingly problematic both from the point of view of environmental emissions and energy sustainability. As an alternative to fossil fuels, hydrogen is widely regarded as a key element for a potential energy solution. In this respect, hydrogen storage technology is considered a key roadblock towards the use of H_2 as an effective energy carrier. Among the methods available to store hydrogen, solid-state storage appears to be the most attractive alternative. This is mostly due to its high safety and volumetric energy density.

Due to their high hydrogen content, tetrahydroborates $M(BH_4)_x$ and their application as hydrogen carriers have been subject of intense studies since the beginning of the last century [1e6]. Although this class of hydrides has been known for a long time, they were initially not considered suitable for reversible hydrogen storage purposes. This lack of initial interest can be traced to their apparent irreversibility. In fact, the products of their thermally activated hydrogen desorption could not be rehydrogenated, unless very harsh conditions were applied [7,8]. In addition, though the possibility to employ them as “one pass” hydrogen storage system was widely investigated, the on-board irreversibility of the hydrogenation process made these materials not suitable for automotive applications. Recently, based on the unexpected kinetic effects of the MgB_2, Barkhordarian et al. [9,10] and Vajo et al. [11,12] reported on the possibility to reversibly store hydrogen in tetrahydroborates when mixed with MgH_2. As confirmed by the numerous works published in the last years, this discovery ignited new interest in this class of hydrides as potential hydrogen storage material. In particular the systems $LiBH_4$eMgH_2 [9,13e19], $Ca(BH_4)_2$eMgH_2 [20,21] and $NaBH_4$eMgH_2 [9,22e31] have been subject of intensive investigations. Among these mixed hydride systems $NaBH_4$eMgH_2 in the molar ratio of 2$NaBH_4$/MgH_2 is considered as a model system for the study of the hydrogen sorption properties. This system is expected to reversibly exchange an amount of hydrogen equal to 7.8 wt.% according to the following reaction: 2$NaBH_4$þMgH_2 4 2NaH þ MgB_2þ4H_2. According to the data available in literature, the overall enthalpy of this reaction is calculated to be 62 kJ mol $^1H_2$ [25,30]. This value entails for the system 2$NaBH_4$þMgH_2 an equilibrium hydrogen pressure of 1 bar at 350 C. Lately, the reaction mechanism of the hydrogen absorption and desorption has been investigated in detail [25,30]. It was reported that the reaction paths of both the hydrogen absorption and desorption take place in several steps. The effect of the $NaBH_4$/MgH_2 ratio on the desorption properties of the system $NaBH_4$eMgH_2 has been also studied. In this regard, Czujko et al. [32] and Garroni et al. [24] observed a marked dependency of the $NaBH_4$ desorption temperature on the

fraction of MgH_2 contained in the system. At the best of our knowledge, no description of the influence of starting reactants ratio on the hydrogen absorption properties exists for the system NaHeMgB_2. Aiming to shed more light on this issue, the hydrogen absorption behavior of the system xNaH þ MgB_2 in the molar ratios 2NaH/ MgB_2, 1.5Na/MgB_2, NaH/MgB_2 and 0.5NaH/MgB_2 were investigated by means of volumetric, HP-DSC, infrared spectroscopy and in situ / ex situ XRD techniques.

2. Experimental

NaH (95% purity) and MgB_2 (99.99% purity) were purchased from SigmaeAldrich and Alfa Aesar, respectively. NaH and MgB_2 were charged into a hardened steel vial and milled for 1 h in a Spex 8000 ball mill, with a ball to powder ratio of 10:1. Handling and milling was performed in a dedicated glove box under a continuously purified argon atmosphere. Ex situ powder Xray diffraction analyses (PXD) were carried out with a Siemens D5000 X-ray diffractometer, using Cu Ka radiation. The powder was spread onto a silicon single crystal and sealed in the glove box with an airtight hood of Kapton foil. Ex situ powder X-ray diffraction analyses (PXD) were carried out also at the MAX II Synchrotron, at beamline I711 in the research laboratory MAX-lab, Lund. The material was charged in a glass capillary and sealed with grease inside a glove box under a continuously purified argon atmosphere. The selected wavelength was 0.939 A.

The in situ Synchrotron Radiation Powder X-ray diffraction (SR-PXD) measurement was performed at the DESY synchrotron, at the beamline D3, Hamburg, Germany. The selected wavelength was 1.097 A. The diffraction patterns measured at the synchrotron facilities were acquired in Debye-Scherrer (transmission) geometry using large area CCD detectors. A special sample holder designed for in situ monitoring of solid/ gas reactions was utilized [13,33,34]. The in situ SR-PXD measurement was performed heating the material from room temperature up to 350 C using a heating rate of 5 C/min. All the raw SR diffraction data were elaborated and converted to powder patterns by the use of FIT2D program [35]. The absorption reactions of the systems xNaH þ MgB_2 were investigated also by high pressure differential scanning calorimetry (HP-DSC, Netzsch DSC 204 HP Phoenix). The HP-DSC measurements were carried out at the constant hydrogen pressure of 50 bar using a heating rate of 5 C/min. The HP-DSC apparatus was placed in a dedicated glove box under a continuously purified argon atmosphere. Volumetric measurements were performed using a Sievert's type apparatus (Hera, Quebec, Canada). The material was heated up to the final temperature of 400 C under a hydrogen pressure of 50 bar using a heating rate of 3 C/min. Temperature programmed desorption (TPD) were also carried out using an Advanced Materials volumetric instrument. The TPD measurements were performed at the constant hydrogen pressure of 50 bar, heating the material from room temperature up to 450 C and then cooling it down to room temperature again (heating/ cooling rate of 5 C/min). Infrared (IR) spectra were recorded using an attenuated total reflection (ATR) setup with a diamond crystal. IR intensities were recorded in the whole wave number range from 400 to 4000 cm^{1} with a nominal resolution of 2 cm^{-1}.

3. Results

Fig. 1 shows the absorption measurements performed for the compositions 2NaH/MgB_2 (A), 1.5Na/MgB_2 (B), NaH/MgB_2 (C) and 0.5NaH/MgB_2 (D) using a Hera volumetric apparatus. The absorption reaction of the system 2NaH/MgB_2 starts at roughly 300 C and continues until an amount of approximately 0.6 wt.% of hydrogen is stored in the system. Then a second reaction step starts and continues to absorb hydrogen for additional 16 h. The final amount of absorbed hydrogen was 5.1 wt.%. The observed absorption reaction for the system 1.5Na/MgB_2 (Fig. 1B) traces out the reaction kinetics observed for the system 2NaH/MgB_2 (Fig. 1A). The measurement was stopped after 21 h and the final amount of hydrogen stored in the system was 4.1 wt.%. The observed absorption reaction for the system NaH/MgB_2 (Fig. 1C) is divided in two steps. In the first step again around 0.6 wt.% of H_2 is stored. During the second step further 4.5 wt.% of H_2 is absorbed. Finally, after 21 h, a final amount of stored hydrogen equal to 5.1 wt.% was achieved. The last investigated system was 0.5NaH/MgB_2 (Fig. 1D). Here again the absorption reaction consists of two steps. In the first step the system charged roughly 0.6 wt.% of hydrogen. Then the absorption reaction continues storing in

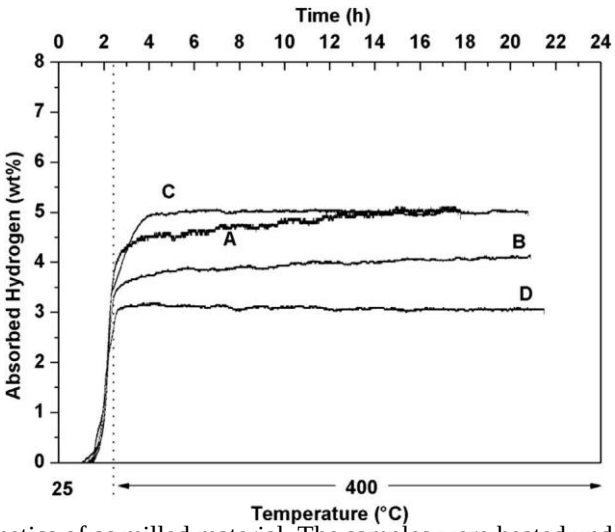

Fig. 1 e Absorption kinetics of as milled material. The samples were heated under 50 bar hydrogen pressure from RT to 400 C (heating rate 3 C/min): (A) 2NaH D MgB_2, (B) 1.5NaH D MgB_2, (C) NaH D MgB_2, (D) 0.5NaH D MgB_2.

the second step further 2.5 wt.% of H_2. The absorption reaction was stopped after about 21 h, when the hydrogen stored in the system was equal to 3.1 wt.%.

In order to understand whether the presence of the two reaction steps is related to real physical phenomena and not to an artifact, the absorption reactions of the xNaH þ MgB_2 mixtures were investigated further by means of thermal programmed treatment technique (Fig. 2(a)). Differently from the volumetric measurements performed with the Hera apparatus, these measurements were carried out heating the samples from room temperature up to 450 C and then cooling it down to near room temperature again using a heating/ cooling rate of 5 C/min. The applied hydrogen pressure was again 50 bar. The obtained absorption profiles were then derived as a function of temperature (Fig. 2(b)). In Fig. 2(a) the hydrogen absorption curves measured for the mixtures 2NaH/ MgB_2 (A), 1.5Na/MgB_2 (B), NaH/MgB_2 (C) and 0.5NaH/MgB_2 (D) are reported. Although, the different heating conditions applied for the TPD measurements lead to hydrogen contents different from those measured in the Hera apparatus (Fig. 1), the derivatives of the absorption profiles (Fig. 2(b)) show an identical number of reaction steps.

The XRD patterns of the as milled 2NaH/MgB_2, 1.5NaH/ MgB_2, NaH/MgB_2 and 0.5NaH/MgB_2 are reported in Fig. 3 (pattern A, B, C and D, respectively). The four xNaH þ MgB_2 specimens show only the presence of NaH and MgB_2 phases. This indicates that additional crystalline phases are not formed during milling. In order to further understand the possible effects of the different NaH/MgB_2 ratios on the hydrogen sorption properties, the diffraction patterns of Fig. 3 were investigated by Rietveld's method. The material crystallite sizes and microstrain for the four xNaH þ MgB_2 compositions are reported in Table 1. Interestingly, as a consequence of the reduced amount of NaH contained in the xNaH þ MgB_2 system, the crystallite size of both NaH and MgB_2 phase decreases. In fact, the measured NaH crystallite size for the system 2NaH/MgB_2 is 629 (31) A, whereas it is 557 (28) A for 1.5NaH/MgB_2, 500 (23) A for NaH/MgB_2 and 496 (26) A for 0.5NaH/MgB_2. The crystallite size of the MgB_2 measured for the system 2NaH/MgB_2 is 383 (19) A and it decreases to 377 (19) A for 1.5NaH/MgB_2, 331 (15) A for NaH/MgB_2 and 269 (14) A for 0.5NaH/MgB_2. The crystallite size decrement of both NaH and MgB_2 indicates a progressive improvement of the ball milling grain refinement efficiency, what appears to be a consequence of the reduction of the NaH amount contained in the xNaH þ MgB_2 mixture. The microstrain of NaH and MgB_2 appears almost constant during milling. The measured microstrain values for NaH are 0.00429 2NaH/MgB_2, 0.00405 for 1.5NaH/MgB_2, 0.00417 for NaH/MgB_2 and 0.00432 for 0.5NaH/ MgB_2. The measured microstrain values for the MgB_2 are 0.00264 for 2NaH/MgB_2, 0.00282 for 1.5NaH/MgB_2, 0.00261 for NaH/MgB_2 and 0.002515 for 0.5NaH/MgB_2. The error associated to the microstrain measurements is roughly the 5%.

The XRD analysis of the materials after hydrogen absorption is presented in Fig. 4. Pattern A shows the presence of $NaBH_4$ together with $NaMgH_3$, free Mg and a small amount of

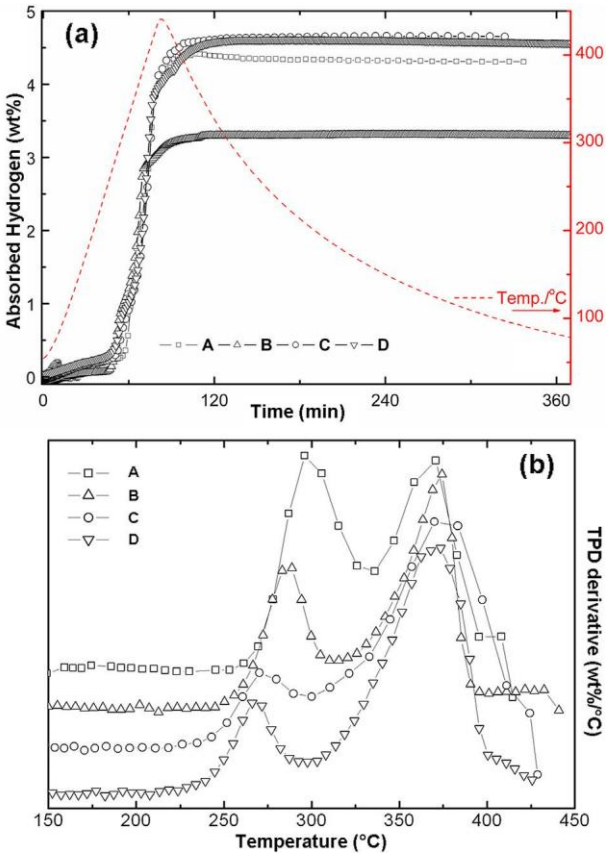

Fig. 2 e (a) Thermal programmed treatment profiles measured at 50 bar of H_2 of the 2NaH D MgB_2 absorption reaction (trace A), 1.5NaH D MgB_2 absorption reaction (trace B), NaH D MgB_2 absorption reaction (trace C) and of 0.5NaH D MgB_2 absorption reaction (trace D), heated from RT to 450 C and subsequently cooled (5 C/min heating/ cooling rate). (b) Derivative of the thermal programmed treatment signals as a function of temperature.

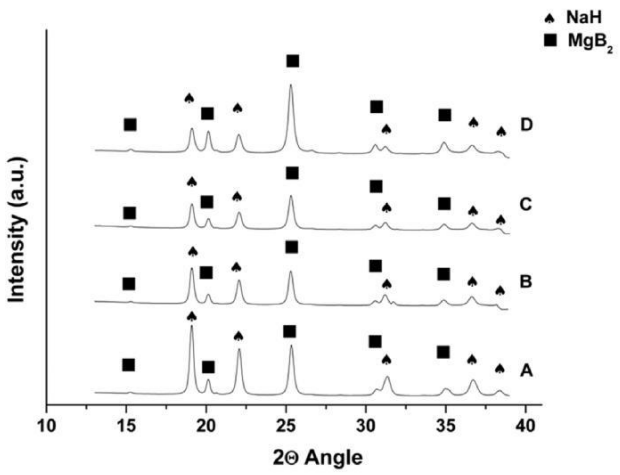

Fig. 3 e PXD patterns of the systems xNaH-MgB_2 as milled: 2NaH/MgB_2, 1.5NaH/MgB_2, NaH/MgB_2, 0.5NaH/MgB_2 (respective patterns A, B, C and D, wavelength [0.939 A).

unreacted NaH and MgB_2 in the hydrogen charged 2NaH/MgB_2 system. Interestingly, MgH_2 does not appear among the final absorption products. The XRD pattern of the hydrogenated 1.5NaH/MgB_2 is shown in Fig. 4B. This sample contains $NaBH_4$, $NaMgH_3$, MgH_2, free Mg and MgB_2. Contrarily to the previously measured samples, the absorbed NaH/MgB_2 (Fig. 4C) does not contain free Mg but MgH_2 together with $NaBH_4$ and MgB_2. A last XRD analysis was performed on the absorbed 0.5NaH/ MgB_2 (Fig. 4D). Similarly to the system NaH/MgB_2, this material shows the presence of free MgH_2, $NaBH_4$ and MgB_2. It should be mentioned that the increasing fraction of unreacted MgB_2 observed respectively in the patterns B, C, D is caused by the different ratio between NaH and MgB_2 in the starting reactants. The XRD analysis shown in Fig. 4 provides information regarding the formation during hydrogen absorption of crystalline phases. The formation of possible amorphous phases during hydrogenation was investigated by IR technique (Fig. 5). The IR spectra of the hydrogenated 2NaH/MgB_2, 1.5NaH/MgB_2, NaH/MgB_2 and 0.5NaH/MgB_2 are A, B, C and D, respectively. For all four samples the absorption bands of $NaBH_4$ are clearly visible. A clear attribution of the other observed absorption bands to the starting reactants and or reaction products is difficult.

In order to visualize the sequence of events taking place during the heating of the systems xNaH þ MgB_2 in hydrogen pressure, HP-DSC analyses were performed. Fig. 6 shows the

Table 1 e Crystallite size of the systems xNaH D MgB_2 as _ milled.

Material	Crystallite size NaH (A)/microstrain (%) [a]	Crystallite size MgB_2 (A)/microstrain (%) [a]
2NaH þ MgB_2	629 (31)/0.00429	383 (19)/0.00264
1.5NaH þ MgB_2	557 (28)/0.00405	377 (19)/0.00282
NaH þ MgB_2	500 (23)/0.00417	331 (15)/0.00261
0.5NaH þ MgB_2	496 (26)/0.00432	269 (14)/0.00251

[a] The errors associated to the microstrain values are about 5%.

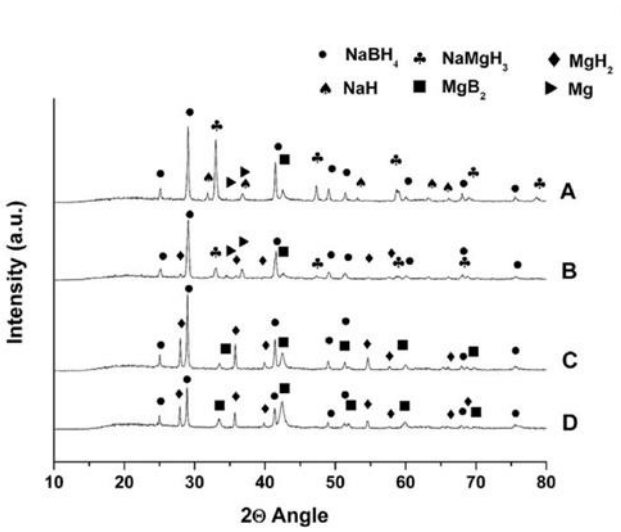

Fig. 4 e PXD patterns of the systems xNaH-MgB_2 hydrogenated under 50 bar and 400 C: 2NaH/MgB_2, 1.5NaH/MgB_2, NaH/MgB_2, 0.5NaH/MgB_2 (respective patterns A, B, C and D, wavelength [1.54184 A).

HP-DSC curves for the following compositions: 2NaH/MgB_2 (curve A), 1.5Na/MgB_2 (curve B), NaH/MgB_2 (curve C) and 0.5NaH/MgB_2 (curve D), measured from room temperature to 400 C and then cooled down to room temperature (constant heating/cooling rate 5 C/min) at 50 bar hydrogen pressure. Although the HP-DSC analysis of the system 2NaH/MgB_2 was discussed in a previous publication [30], a further measurement was made and here reported for comparison purposes. The HP-DSC curve recorded for the system 1.5Na/MgB_2 shows a trend similar to that observed for the system 2NaH/MgB_2. However, slight differences can be noticed. The position of the first exothermic peak during heating is shifted by 6 C towards lower temperatures (onset temperature 271 C) with respect to the observed signal in the reference system 2NaH/MgB_2 (onset temperature 277 C). Although under heating also other signals undergo shift to lower temperature, the magnitude of those shifts is smaller than 5 C. The cooling period of the HP-

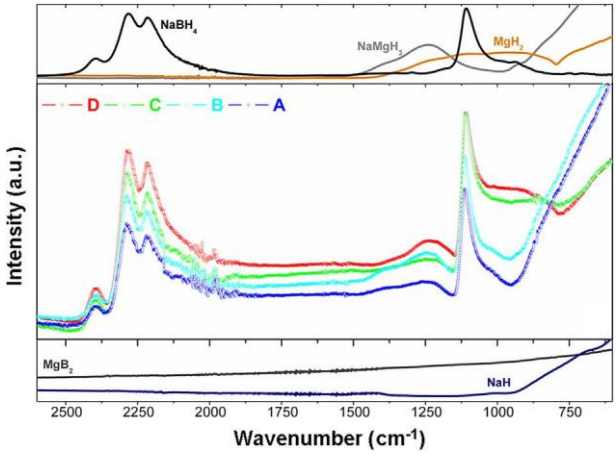

Fig. 5 e IR spectra of the systems xNaH D MgB_2 hydrogenated under 50 bar and 400 C.

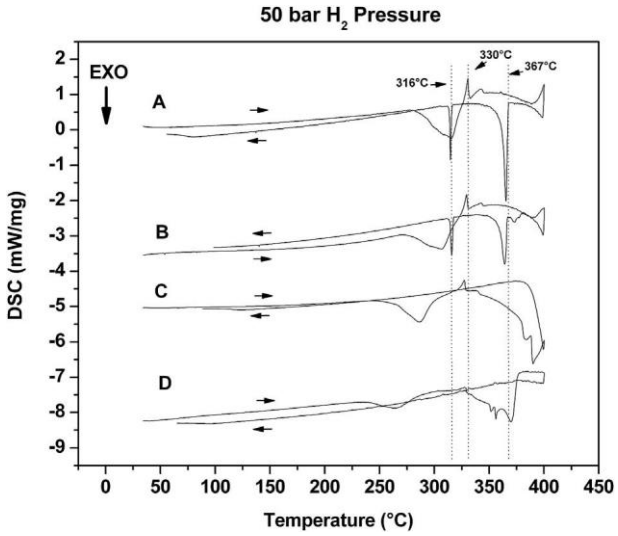

Fig. 6 e HP-DSC curves measured at 50 bar of H_2 of the 2NaH D MgB_2 absorption reaction (curve A), 1.5NaH D MgB_2 absorption reaction (curve B), NaH D MgB_2 absorption reaction (curve C) and of 0.5NaH D MgB_2 absorption reaction (curve D), measured from RT to 400 C and subsequently cooled (5 C/min heating/cooling rate).

DSC curve B is characterized by the presence of two main exothermic peaks at 367 C and 317 C plus another smaller exothermic peak at 380 C. The HP-DSC analysis of the system NaH/MgB_2 shows during heating a first exothermic event at 248 C, followed by a small endothermic signal with maximum at 328 C and by a broad exothermic signal split into two parts starting at 330 C. In contrast to the previous measurements, the cooling period does not show any hint for ongoing reactions. Finally, the composition 0.5NaH/MgB_2 was also investigated by means of HP-DSC technique. A first exothermic signal at 240 C and a small endothermic peak at 328 C are visible. These signals are followed by a broad exothermic peak at 320 C split into three parts with maxima at 352 C, 356 C and 370 C. Because of the overlaps between them, it is not possible to give precise onset temperatures. Similarly to the system NaH/MgB_2, also here the cooling period is characterized by the absence of detectable events.

In order to better understand the effect of the NaH/MgB_2 ratio on the hydrogen absorption reaction, the hydrogenation reaction of the system 0.5NaH/MgB_2 was further characterized by in situ SR-PXD analysis (Fig. 7). The measurement was carried out at 50 bar of hydrogen pressure, in scanning temperature from RT to 350 C and then keeping the system under isothermal conditions at 350 C for several minutes. The phases in the starting materials are NaH and MgB_2. During heating, at roughly 230 C, the appearance of a boron-based phase recently described in another work is observed [36]. Later on, at 270 C, the appearance of this phase is followed by the formation of $NaMgH_3$. With the appearance of the $NaMgH_3$ phase, the NaH phase disappears completely. At 325 C the formation of $NaBH_4$ and little later MgH_2 is observed together with the simultaneous disappearance of both $NaMgH_3$ and the boron-based phase. In contrast to the system 2NaH/MgB_2 [30] the system 0.5NaH/MgB_2 (Fig. 7) does not show the formation of an amorphous background. In addition, the formation of MgH_2 was achieved.

Due to the kinetic constrains observed during the hydrogenation of the system 2NaH þ MgB_2, the mixtures with a NaH/MgB_2 ratio higher than 2:1 were not investigated; however, the system 3NaH þ MgB_2 appears promising. In fact, assuming a complete conversion of NaH and MgB_2 into $NaBH_4$ and $NaMgH_3$, this system has a theoretical gravimetric hydrogen capacity of 6.4 wt.%. In addition, based on the thermodynamic data reported on the HSC Chemistry 6.12 database, the calculated equilibrium pressure of the system 3NaH þ MgB_2 is 1 bar H_2 at 320 C (30 C lower than that of 2NaH/MgB_2). This temperature value is particularly interesting because it lies much below the observed melting point of the NaHeNaBH$_4$ eutectic mixture (383 C). Therefore, it might be possible to perform both absorption and desorption measurements avoiding the kinetic constrains related to the formation of the eutectic molten phase [37].

4. Discussion

In the results section, the absorption reaction mechanism of the system xNaH þ MgB_2 at a pressure of 50 bar H_2 was shown to strongly depend on the NaH/MgB_2 ratio of the starting material. This effect is clearly visible in the volumetric analysis of Fig. 1. In fact, though all measured absorption kinetics show a similar first absorption step, they strongly differ in the manner the hydrogen absorptions proceeds. In particular, sensible differences are observed between the systems 2NaH/ MgB_2 and 0.5NaH/MgB_2 (Fig. 1 curves A and D), whereas the absorption curves of the systems 1.5NaH/MgB_2 and 1NaH/ MgB_2 are rather similar to those of 2NaH/MgB_2 and 0.5NaH/ MgB_2, respectively. Differences are also visible in the XRD analysis of the absorbed materials (Fig. 4). The absorbed 2NaH/ MgB_2 and 1.5NaH/MgB_2 (pattern A and B) show both the presence of $NaMgH_3$, free Mg and MgB_2 among the reaction products. The absorbed NaH/MgB_2 and 0.5NaH/MgB_2 (pattern C and D) are composed of $NaBH_4$, MgH_2 and MgB_2.

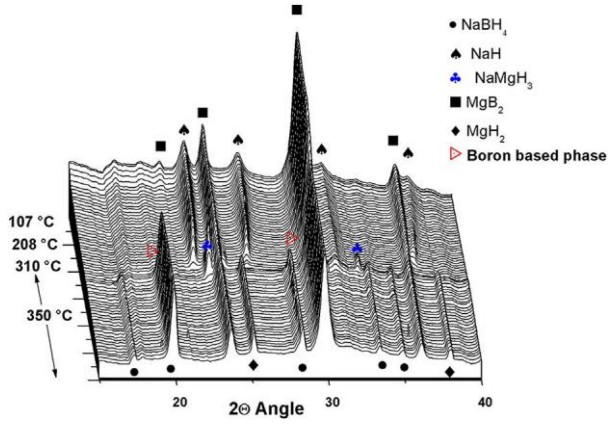

Fig. 7 e Series of SR-PXD patterns of the 2NaH D MgB_2 system heated at 50 bar hydrogen pressure from RT to 350 C and kept under isothermal condition (5 C/min, wavelength [1.097 A).

The IR analyses reported in Fig. 5 show for all the investigated samples the presence of the absorption bands of $NaBH_4$. The absence of absorption bands different from those of $NaBH_4$ hints at the absence of other phases containing covalent bonds (e.g. BeH bonds). As written in the results section an attribution of the IR signals observed in Fig. 5 to the other phases observed in the PXD patterns shown in Fig. 4 is difficult. This is due to the ionic character of the bonds present in the NaH, $NaMgH_3$, MgH_2 and MgB_2.

Clear differences between the absorption reactions of the different systems are also visible in the calorimetric analyses presented in Fig. 6 (curve A, B, C and D). The onset temperature of the first exothermic peak of the curves B, C and D (peaks attributed to the formation of the boronbased phase and the $NaMgH_3$ phase [30]) following the decrement of the NaH amount, sensibly shifts towards lower temperature. This indicates a direct relation between the earlier beginning of the absorption reaction and the amount of NaH contained in the system. The amount of energy transferred to the powder during milling is independent from the powder composition and therefore equal for all the batches of material prepared, however, the decrement of the NaH fraction contained in the system and consequent increment of the MgB_2 fraction might sensibly influence the milling process. Magnesium diboride it's a ceramic material with a high hardness, therefore, during milling the increment of the MgB_2 portion leads to an enhancement of the NaH and MgB_2 crystallite size refinement. The data reported in Table 1 confirms that the crystallite size of both NaH and MgB_2 in the milled material decreases reducing the amount of the NaH in the xNaH þ MgB_2 system. This phenomenon clearly leads to a shortening of the paths which the diffusing species have to overcome in order to form the hydrogenated products. Therefore, as result of the diffusion distances shortening, the onset temperature of the hydrogen absorption reaction is lowered. This is also valid for the $NaBH_4$ formation. In fact, in the case of the system 0.5NaH/MgB_2 the formation of the $NaBH_4$ starts at 325 C (Fig. 6), which is about 30 C lower than in the reference system 2NaH/MgB_2. A further effect of the lower amount of NaH is observed in the HP-DSC analysis shown in Fig. 4, where an intensity drop of the endothermic signal related to the melting of the boron-based phase at 330 C [30] is observed. This decrement, particularly significant for the composition NaH/MgB_2 and 0.5NaH/MgB_2 (Fig. 6C and D, respectively), occurs most likely due to the fact that the boron-based phase and $NaMgH_3$ start to be consumed before the temperature reaches 330 C. The boron-based phase consumption during the heating of the

material explains also the absence of the exothermic peak during the cooling at 316 C in the HP-DSC curves C and D (Fig. 6).

In the range of temperature between 330 C and 400 C, the absorption reaction mechanisms of the four investigated stoichiometries reveal further differences. Similarly to the endothermic signal at 330 C these differences are more marked in the case of the systems NaH/MgB_2 and $0.5NaH/ MgB_2$ (Fig. 6C and D). In fact, whereas for the systems $2NaH/ MgB_2$ and $1.5NaH/MgB_2$ (Fig. 6A and B) only a single exothermic signal is visible, the systems NaH/MgB_2 (Fig. 6C) and $0.5NaH/MgB_2$ (Fig. 6D) show the presence of a broad peak split into two and three parts, respectively. These differences in respect to the reference system $2NaH/MgB_2$ are due to the continued hydrogen absorption reaction towards the forma-tion of $NaBH_4$, MgH_2 and disappearance of $NaMgH_3$ which takes place in multiple steps as clearly visible in the SR-PXD analysis of Fig. 7. In addition, the absence of additional peaks in the cooling period of the curves C and D of Fig. 6 is an evidence of the completeness of the absorption reaction (Fig. 4). As already mentioned, differently from the system $2NaH/MgB_2$, the absorption reaction performed for $0.5NaH/ MgB_2$ (Fig. 7) does not lead to the formation of the $NaHeNaBH_4$ molten phase [30]. This is due to the fact that in the system $0.5NaH/MgB_2$ the formation of $NaBH_4$ starts after NaH is completely consumed by the previous formation of $NaMgH_3$. According to what was observed in our previous work, the presence of the $NaBH_4$eNaH molten phase might affect the hydrogen diffusion in the system. This hypothesis is confirmed by the fact that for the system $0.5NaH/MgB_2$ (where the formation of the $NaHeNaBH_4$ molten phase is not observed) the absorption reaction continues towards the formation of $NaBH_4$ and MgH_2. The absorption reaction mechanism for the system $0.5NaH/MgB_2$ under a hydrogen pressure of 50 bar heating the material from room temperature up to 400 C can be reassumed as it follows: upon heating at roughly 230 C a boron-based phase is formed. The formation of this phase is followed by the formation of $NaMgH_3$ at 270 C. Simultaneously with the formation of $NaMgH_3$, NaH is completely consumed. In the range of temperature between 325 and 370 C the formation of $NaBH_4$ and little later MgH_2 is observed together with the simultaneous disappearance of both $NaMgH_3$ and the boron-based phase.

The absorption measurements performed at 50 bar pressure for the systems NaH/MgB_2 and $0.5NaH/MgB_2$ show a hydrogen uptake slightly lower than the theoretical values (5.4 and 3.36 wt.%, respectively). This can be explained by possible material losses on the sample holder walls and to partial segregation of the starting reactants and products during hydrogenation. The partial segregation of components of the system is due to the presence during heating of portion of material in different states (i.e. liquid and solid). In fact although in the range of temperature investigated in this work MgB_2, MgH_2 and $NaMgH_3$ are solid NaH and $NaBH_4$ go trough molten states.

5. Conclusions

In this work the effect of the ratio between NaH and MgB_2 on the absorption reaction of the system $NaHeMgB_2$ was investigated by means of volumetric methods, in situ/ex situ PXD, calorimetric and IR techniques. It was found that during milling the reduction of the amount of the NaH contained in the system $xNaH$ þ MgB_2 leads to a reduction of the crystallite size of both NaH and MgB_2. As results of the crystallite size reduction, the hydrogenation reaction starts earlier. Although, for none of the investigated compositions the theoretical gravimetric hydrogen capacity was achieved, the amount of hydrogen stored in $NaH + MgB_2$ and $0.5NaH + MgB_2$ just slightly differed from the expected values.

Differently from the systems with higher content of NaH, the only crystalline products of the hydrogenation of $NaH + MgB_2$ and $0.5NaH + MgB_2$ are $NaBH_4$ and MgH_2. Due to the reduced amount of NaH in the system $0.5NaH$ þ MgB_2, the hydrogenation reaction proceeds towards the formation of $NaBH_4$ and MgH_2 consuming completely the formed $NaMgH_3$ and avoiding the formation of the molten phase $NaHeNaBH_4$.

Acknowledgments

This work was supported by the European Community under MRTN-Contract “Complex Solid State Reactions for Energy Efficient Hydrogen Storage” (MRTN-CT-2006-035366) and COST Action MP1103.

References

[1] Schlesinger HI, Brown HC, Finholt AE, Gilbreath JR, Hoekstra HR, Hyde EK. Sodium borohydride, its hydrolysis and its use as a reducing agent and in the generation of hydrogen. J Am Chem Soc 1953;75:215e9.

[2] Stander CM. Kinetics of formation of magnesium hydride from magnesium and hydrogen, vol. 104; 1977. pp. 229e38.

[3] Stander CM. Kinetics of decomposition of magnesium hydride. J Inorg Nucl Chem 1977;39:221e3.

[4] Stock A. Hydrides of boron and silicon. New York, Ithaca: Cornell University Press; 1933.

[5] Stock A, Nassenz C. Hydrogen boride. Berichte 1912;45:3539e68.

[6] Zuttel A, Borgschulte A, Orimo SI. Tetrahydroborates as new hydrogen storage materials. Scr Mater 2007;56:823e8.

[7] Dymova TN, Dergachev YM, Sokolov VA, Grechanaya NA. Pressure of $NaAlH_4$ and Na_3AlH_6 dissociation. Dokl Akad Nauk SSSR 1975;224:591e2.

[8] Dymova TN, Eliseeva NG, Bakum SI, Dergache. Ym. Direct synthesis of alkali-metal alumohydrides in melts. Dokl Akad Nauk SSSR 1974;215:1369e72.

[9] Barkhordarian G, Klassen T, Dornheim M, Bormann R. Unexpected kinetic effect of MgB_2 in reactive hydride composites containing complex borohydrides. J Alloy Compd 2007;440:L18e21.

[10] Barkhordarian G, Klassen T, Bormann R. Internetional patent pending ed: WO 2006/063627 A1.

[11] Vajo JJ, Mertens FO, Ahn CC, Bowman RC, Fultz B. Altering hydrogen storage properties by hydride destabilization through alloy formation: LiH and MgH_2 destabilized with Si. J Phys Chem B 2004;108:13977e83.

[12] Vajo JJ, Mertens FO, Skeith SL, Balogh MP. International patent pending ed: WO 2005/097671.

[13] Bosenberg U, Doppiu S, Mosegaard L, Barkhordarian G, Eigen N, Borgschulte A, et al. Hydrogen sorption properties of MgH_2-$LiBH_4$ composites. Acta Mater 2007;55:3951e8.

[14] Bosenberg U, Kim JW, Gosslar D, Eigen N, Jensen TR, von Colbe JMB, et al. Role of additives in $LiBH_4$-MgH_2 reactive hydride composites for sorption kinetics. Acta Mater 2010;58:3381e9.

[15] Bosenberg U, Vainio U, Pranzas PK, von Colbe JMB, Goerigk G, Welter E, et al. On the chemical state and distribution of Zr-and V-based additives in reactive hydride composites. Nanotechnology 2009;20:9.

[16] Deprez E, Justo A, Rojas TC, Lopez-Cartes C, Minella CB, Bosenberg U, et al. Microstructural study of the $LiBH_4$-MgH_2 reactive hydride composite with and without Ti-isopropoxide additive. Acta Mater 2010;58:5683e94.

[17] Deprez E, Munoz-Marquez MA, Roldan MA, Prestipino C, Palomares FJ, Minella CB, et al. Oxidation state and local structure of Ti-based additives in the reactive hydride composite 2LiBH(4) þ MgH_2. J Phys Chem C 2010;114:3309e17.

[18] Vajo JJ, Olson GL. Hydrogen storage in destabilized chemical systems. Scr Mater 2007;56:829e34.

[19] Vajo JJ, Skeith SL, Mertens FO. Reversible storage of hydrogen in destabilized $LiBH_4$. J Phys Chem B 2005;109:3719e22.

[20] Barkhordarian G, Jensen TR, Doppiu S, Bosenberg U, Borgschulte A, Gremaud R, et al. Formation of $Ca(BH_4)_2$ from hydrogenation of CaH_2 þ MgB_2 composite. J Phys Chem C 2008;112:2743e9.

[21] Bonatto Minella C, Garroni S, Olid D, Teixidor F, Pistidda C, Lindemann I, et al. Experimental evidence of Ca[B12H12] formation during decomposition of a $Ca(BH_4)_2$ þ MgH_2 based reactive hydride composite. J Phys Chem C 2011;115:18010e4.

[22] Garroni S, Milanese C, Girella A, Marini A, Mulas G, Menendez E, et al. Sorption properties of NaBH(4)/MH(2) (M ¼ Mg, Ti) powder systems. Int J Hydrogen Energy 2010;35:5434e41.

[23] Garroni S, Milanese C, Pottmaier D, Mulas G, Nolis P, Girella A, et al. Experimental evidence of Na-2[B12H12] and Na formation in the desorption pathway of the
2NaBH(4) þ MgH_2 system. J Phys Chem C 2011;115:16664e71.

[24] Garroni S, Minella CB, Pottmaier D, Pistidda C, Milanese C, Marini A, et al. Mechanochemical synthesis of $NaBH_4$ starting from NaH-MgB_2 reactive hydride composite system. Int J Hydrogen Energy 2013;38:2363e9.

[25] Garroni S, Pistidda C, Brunelli M, Vaughan GBM, Surinach S, Baro MD. Hydrogen desorption mechanism of 2NaBH(4) þ MgH_2 composite prepared by high-energy ball milling. Scr Mater 2009;60:1129e32.

[26] Mao JF, Yu XB, Guo ZP, Liu HK, Wu Z, Ni J. Enhanced hydrogen storage performances of $NaBH_4$-MgH_2 system. J Alloy Compd 2009;479:619e23.

[27] Nwakwuo CC, Pistidda C, Dornheim M, Hutchison JL, Sykes JM. Microstructural study of hydrogen desorption in 2NaBH(4) þ MgH_2 reactive hydride composite. Int J Hydrogen Energy 2011;37:2382e7.

[28] Nwakwuo CC, Pistidda C, Dornheim M, Hutchison JL, Sykes JM. Microstructural analysis of hydrogen absorption in 2NaH þ MgB_2. Scr Mater 2010;64:351e4.

[29] Pistidda C, Barkhordarian G, Rzeszutek A, Garroni S, Minella CB, Baro MD, et al. Activation of the reactive hydride composite 2NaBH(4) þ MgH_2. Scr Mater 2011;64:1035e8.

[30] Pistidda C, Garroni S, Minella CB, Dolci F, Jensen TR, Nolis P, et al. Pressure effect on the 2NaH þ MgB_2 hydrogen absorption reaction. J Phys Chem C 2010;114:21816e23.

[31] Pottmaier D, Pistidda C, Groppo E, Bordiga S, Spoto G, Dornheim M, et al. Dehydrogenation reactions of 2NaBH(4) þ MgH_2 system. Int J Hydrogen Energy 2011;36:7891e6.

[32] Czujko T, Varin RA, Wronski Z, Zaranski Z, Durejko T. Synthesis and hydrogen desorption properties of nanocomposite magnesium hydride with sodium borohydride (MgH_2 þ $NaBH_4$). J Alloy Compd 2007;427:291e9.

[33] Clausen BS, Steffensen G, Fabius B, Villadsen J, Feidenhansl R, Topsoe H. Insitu cell for combined XRD and online catalysis test e studies of Cu-based water gas shift and methanol catalysts. J Catal 1991;132:524e35.

[34] Rodriguez JA, Hanson JC, Frenkel AI, Kim JY, Perez M. Experimental and theoretical studies on the reaction of H-2 with NiO: role of O vacancies and mechanism for oxide reduction. J Am Chem Soc 2002;124:346e54.

[35] http://www.esrf.eu/computing/scientific/FIT2D/.

[36] Pistidda C, Napolitano E, Pottmaier D, Dornheim M, Klassen T, Baricco M, et al. Structural study of a new B-rich phase obtained by partial hydrogenation of 2NaH þ MgB_2. Int J Hydrogen Energy 2013;25:10479e84.

[37] Stasinevich DS, Egorenko GA. Thermographic investigation of alkali metal and magnesium tetrahydroborates at pressures up to 10 atm. Russ J Inorg Chem 1968;13(3):341e3.